Journal of Medicinal Chemistry

Article

pubs.acs.org/jmc

Identification and Preliminary Characterization of a Potent, Safe, and Orally Efficacious Inhibitor of Acyl-CoA:Diacylglycerol Acyltransferase 1

Vince S. C. Yeh, David W. A. Beno, Sevan Brodjian, Michael E. Brune, Steven C. Cullen, Brian D. Dayton, Madhup K. Dhaon, Hugh D. Falls, Ju Gao, Nelson Grihalde, Philip Hajduk, T. Matthew Hansen, Andrew S. Judd, Andrew J. King, Russel C. Klix, Kelly J. Larson, Yau Y. Lau, Kennan C. Marsh, Scott W. Mittelstadt, Dan Plata, Michael J. Rozema, Jason A. Segreti, Eric J. Stoner, Martin J. Voorbach, Xiaojun Wang, Xili Xin, Gang Zhao, Christine A. Collins, Bryan F. Cox, Regina M. Reilly, Philip R. Kym, and Andrew J. Souers*

Global Pharmaceutical Research and Development, Abbott Laboratories, 100 Abbott Park Road, Abbott Park, Illinois 60064-6100, United States

Supporting Information

ABSTRACT: A high-throughput screen against human DGAT-1 led to the identification of a core structure that was subsequently optimized to afford the potent, selective, and orally bioavailable compound **14**. Oral administration at doses ≥0.03 mg/kg significantly reduced postprandial triglycerides in mice following an oral lipid challenge. Further assessment in both acute and chronic safety pharmacology and toxicology studies demonstrated a clean profile up to high plasma levels, thus culminating in the nomination of **14** as clinical candidate ABT-046.

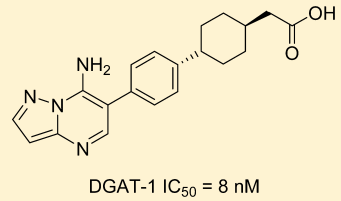

DGAT-1 IC_{50} = 8 nM

INTRODUCTION

Excess accumulation of triglycerides in the blood and in tissues is a hallmark of diverse metabolic disturbances including atherogenic dyslipidemia, insulin resistance, and hepatic steatosis. In addition, deposition of triglycerides in adipose tissue causes obesity, and evidence is mounting that the accumulation of triglycerides in nonadipose tissue is a principal cause of the constellation of cardiovascular risk factors associated with the Metabolic Syndrome.[1] The final and only committed step in the synthesis of triglycerides is common to both major triglyceride biosynthesis pathways and is catalyzed by acyl CoA:diacylglycerol acyltransferase (DGAT) enzymes.[2] This family is comprised of DGAT-1 and DGAT-2, which share limited homology.[3,4]

DGAT-1, in particular, has received significant attention as a therapeutic target for cardiometabolic diseases following the disclosure of the DGAT-1 knockout mice phenotype.[5,6] Mice lacking the DGAT-1 gene were shown to be viable and resistant to the effects of diet-induced obesity (DIO) and hepatic steatosis when fed a high-fat diet. Additionally, these animals were reported to have an increased sensitivity to both insulin and leptin, decreased levels of tissue triglycerides, and increased energy expenditure. Further studies demonstrated that DGAT-$1^{-/-}$ mice had dramatically reduced levels of intestinal triglyceride synthesis and chylomicron secretion following an oral lipid challenge.[7−9]

Since the initial disclosure of DGAT-1 inhibitors by Bayer[10] and the Tularik/Japan Tobacco group,[11] several companies have reported orally active inhibitors of this enzyme that recapitulate several metabolic aspects of the DGAT-$1^{-/-}$ knockout mice.[12] Additionally, Pfizer[13] and Novartis[14] have advanced DGAT-1 inhibitors into the clinic for diabetes and dyslipidemia, respectively; thus, results from larger powered trials may provide human proof of concept for this novel mechanism in the near future.

We previously reported the identification and characterization of compound A-922500 (**1**), which was used as a tool to provide early preclinical validation for the hypothesis that DGAT-1 inhibitors could induce weight loss in DIO mice and lower triglyceride excursions in the postprandial state in multiple rodent models (Figure 1).[15−17] To identify additional pharmacophores that could serve as inhibitors of DGAT-1, we conducted a high-throughput screen (HTS) against a recombinant form of the human enzyme. Compounds **2** and **3** were identified as hits with >50% enzyme inhibition at 10 μM, and subsequent validation experiments determined IC_{50} values of 1.58 and 0.044 μM, respectively. While the more active analogue **3** was rapidly metabolized in human liver microsomes (HLM), we were intrigued by the high binding efficiency (BE) of this compact inhibitor.[18]

The 40-fold increase in enzyme potency of analogue **3** relative to **2** highlighted the critical nature of the fused pyrazolo[1,5-*a*]pyrimidine ring system in the former compound. Additionally, a rapid scan of des-amino, methylamino, and dimethylamino analogues indicated that the exocyclic 7-amino moiety was essential, as all three compounds showed significant diminution of enzyme inhibition (data not shown).

Received: December 2, 2011
Published: January 20, 2012

ACS Publications © 2012 American Chemical Society

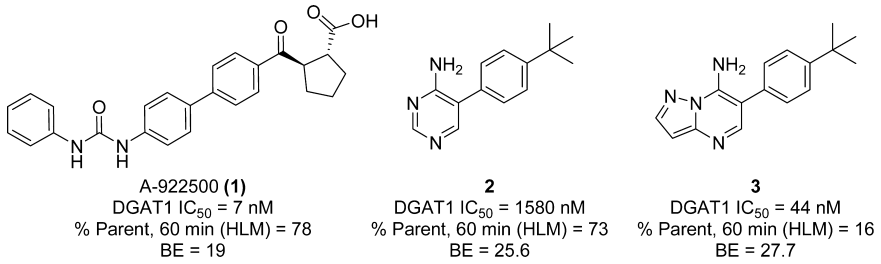

Figure 1. DGAT-1 inhibitor A-922500 (**1**) and two structurally related hits from an HTS against human DGAT-1.

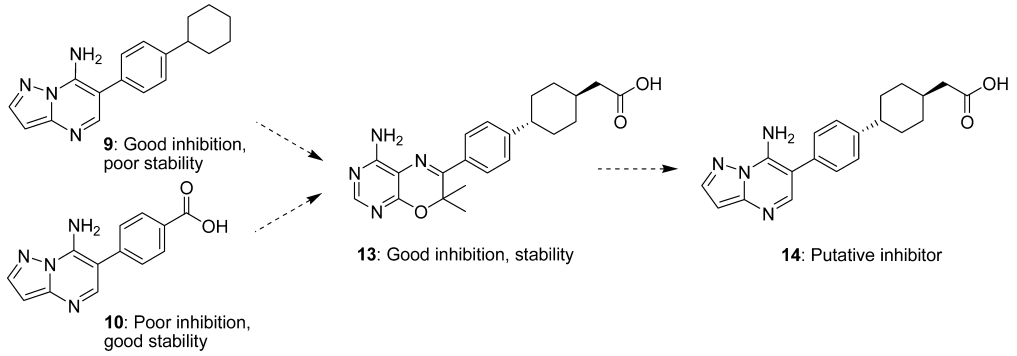

Figure 2. Synopsis of the design of putative DGAT-1 inhibitor **14**.

Table 1. DGAT-1 Inhibition and Microsomal Stability of Selected Compounds[a]

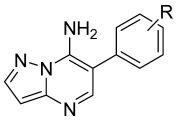

compd	R	hDGAT-1 IC_{50} (μM)[b]	HLM (% parent)[c]
3	4-*tert*-butyl	0.0440	16
4	H	>10.0	ND
5	4-bromo	1.86	<5
6	3-bromo	>10.0	<5
7	2-bromo	>10.0	69
8	4-isopropyl	0.250	<5
9	4-cyclohexyl	0.110	ND
10	4-carboxylic acid	>10.0	100
11	4-methylsulfone	>10.0	91

[a]All compounds were >95% pure by HPLC and characterized by ^{1}H NMR and MS. [b]Values are the means of a series of separate assays, each performed in triplicate. [c]60 min. ND, not determined.

This prompted us to retain the 6-phenylpyrazolo[1,5-*a*]-pyrimidin-7-amine pharmacophore as a starting point for optimization while rapidly probing the importance of the hydrophobic *tert*-butyl moiety. To this end, we prepared the nonsubstituted phenyl analogue **4**, as well as analogues with a simple hydrophobe (bromine) placed systematically around the terminal phenyl ring. As shown in Table 1, phenyl analogue **4** was inactive against DGAT-1, as were the *meta*-bromo and *ortho*-bromo substituted analogues **6** and **7**. The *para*-bromo analogue **5** showed an IC_{50} of 1.86 μM, thus confirming the preference for substitution at this position. In HLM, the metabolic stabilities of these compounds were similar or worse than the hit structure **3**, with the interesting exception of *ortho*-bromo-substituted analogue **7**.

We next performed a rapid scan of analogues with hydrophobic and hydrophilic substitutions at the *para* position (Table 1). Substitution of a terminal isopropyl group for the *tert*-butyl moiety in **3** lead to an approximately 6-fold decrease in DGAT-1 inhibition (**8**), whereas the cyclohexyl derivative (**9**) was within 2-fold of analogue **3**. Similar to the parent structure, both analogues possessed very poor metabolic stability in HLM. While analogues with ionizable (**10**) or polarizeable (**11**) groups at the *para* position were devoid of DGAT-1 inhibition, both carboxylic- and sulfone-containing moieties conferred excellent stability in HLM, thus indicating the beneficial effect of increased polarity on this metabolic parameter.[19]

Given the clear requirements of hydrophobic *para*-substitution for obtaining good enzyme inhibition and polar terminal substitution for obtaining acceptable microsomal stability, we were intrigued by the possibility of merging these two structural features via an extended linker region to afford putative inhibitor **14** (Figure 2).[20] This was additionally inspired by the literature compound **13**, which was first disclosed in 2004 by the Tularik/Japan Tobacco group and has

dx.doi.org/10.1021/jm201524g | J. Med. Chem. 2012, 55, 1751–1757

subsequently served as the structural foundation of multiple series from other companies.[13,21]

CHEMISTRY

Analogues **3**–**11** were prepared according to Scheme 1. Briefly, known benzyl nitriles (**12**, Scheme 1) were condensed with

Scheme 1. [a]

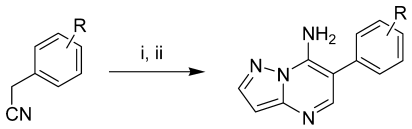

[a](i) 2-*tert*-Butoxy-*N*,*N*,*N*′,*N*′-tetramethylethane-1,1-diamine, toluene, reflux. (ii) 3-Aminopyrazole, HOAc, toluene, reflux.

Bredereck's reagent in toluene and subsequently condensed with 3-aminopyrazole.

The synthesis of compound **14** (Scheme 2) was initiated via Horner–Wadsworth–Emmons olefination of 4-phenylcyclohexanone to afford the α,β-unsaturated ester **15**. Subsequent hydrogenation afforded intermediate **16a** as a mixture of isomers (2.4/1, *trans*/*cis*). Following saponification, the *trans* isomer was then preferentially crystallized as a lithium salt and re-esterified to provide pure ester **16b** in 60% yield. Friedel–Crafts acylation afforded the corresponding acid chloride, which was hydrogenated over palladium on carbon to furnish the benzylic alcohol **17**. Subsequent bromination and displacement via sodium cyanide provided nitrile **18** in 80% yield. Condensation with Bredereck's reagent in refluxing toluene followed by a second condensation with 2-amino pyrazole afforded the penultimate ester **19**. Finally, base-mediated ester hydrolysis and acidification furnished the desired analogue **14** in 76% yield.

RESULTS AND DISCUSSION

As shown in Table 2, hybrid structure **14** showed potent inhibition against both human and mouse isoforms of DGAT-1 (IC_{50} = 8 nM) and retained much of the high BE (BE = 23.1) of hit structure **3**. Additionally, this compound showed no inhibition against human DGAT-2 and inhibited triglyceride formation in HeLa cells expressing human DGAT-1 with an IC_{50} of 78 nM. Compound **14** demonstrated negligible turnover in microsome preparations from mouse and human livers, indicating that the hybrid design conferred both potent enzyme inhibition and microsomal stability. Finally, **14** exhibited high in vitro permeability values in Caco-2 cells with no evidence of active efflux (efflux ratio = 1.4 and 1.1 at 0.5 and 5 μM, respectively).

We next assessed the pharmacokinetic properties of **14** in mouse and rat in advance of acute efficacy studies (Table 3). The properties following a single intravenous dose were characterized by low volumes of distribution and plasma clearance values and moderate terminal plasma elimination half-lives of 4.6 and 3.8 h in mouse and rat, respectively. The oral absorption was high for both species, affording excellent levels of bioavailability.

To investigate the in vivo effects of specific inhibition of intestinal DGAT-1, compound **14** was evaluated in a model of postprandial hyperlipidemia measuring chylomicron-derived triglycerides. CD-1 mice were fasted overnight and then administered a single dose of 0.03, 0.3, or 3 mg/kg via oral gavage. One hour later, the mice were given an oral corn oil bolus (6 mL/kg), and serum triglycerides and drug concentrations were measured after 2 h. As demonstrated in Figure 3A, **14** showed a dose-dependent reduction in serum triglycerides starting at 0.03 mg/kg and increasing through the higher doses (40, 60, and 90% reduction from vehicle at 0.03, 0.3, and 3.0 mg/kg, respectively). The ascending pharmacodynamics correlated well with a linear increase in plasma exposure going from 0.03 to 3 mg/kg (C_{2h} = 0.033, 0.36, and 3.10 μg/mL at 0.03, 0.3, and 3.0 mg/kg, respectively).

We subsequently measured the ability of DGAT-1 inhibitor **14** to reduce serum triglycerides throughout the time span covering the postprandial excursion in DIO mice. A dose of 0.3 mg/kg, which showed significant efficacy in nonobese CD-1 mice, was chosen. One hour after oral dosing of the DGAT-1 inhibitor, a corn oil bolus (6 mL/kg) was administered, and serum triglycerides subsequently were measured each hour for

Scheme 2. [a]

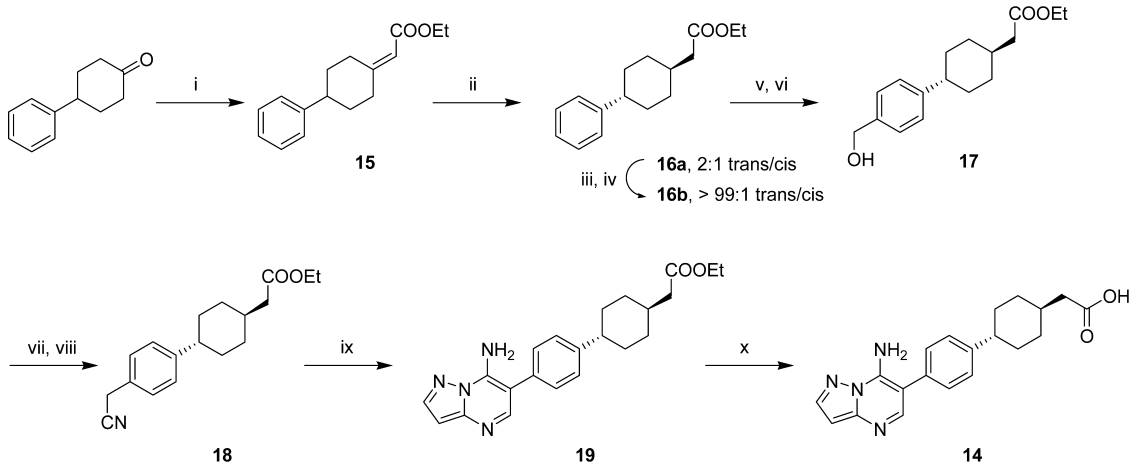

[a](i) Triethyl phosphonoacetate, NaO*t*Bu, THF. (ii) H_2, Pd(C), EtOH. (iii) LiOH, EtOH/H_2O. (iv) EtOH, H_2SO_4. (v) $AlCl_3$, oxalyl chloride, DCM. (vi) H_2, Pd (C), TEA, THF. (vii) HBr, HOAc. (viii) NaCN, ACN/water, 40 °C. (ix) 2-*tert*-Butoxy-*N*,*N*,*N*′,*N*′-tetramethylethane-1,1-diamine, toluene, reflux and then 3-aminopyrazole, HOAc, toluene, reflux. (x) NaOH, MeOH, THF, 50 °C.

dx.doi.org/10.1021/jm201524g | J. Med. Chem. 2012, 55, 1751–1757

Table 2. Selected Enzyme Inhibition and in Vitro ADME Results for Compound 14

DGAT IC_{50} (nM)[a]			triglyceride synthesis IC_{50} (nM)[ab]	microsomal stability (% parent)[c]		permeability[d]
hDGAT-1	mDGAT-1	hDGAT-2	HeLa cells	HLM	MLM	Caco-2 (cm/s)
8	8	>10000	78	97	99	84×10^{-6}

[a]Values are the means of a series of separate assays, each performed in triplicate. [b]Inhibition of triglyceride synthesis determined in HeLa cells. See the Supporting Information for experimental details and references. [c]60 min. [d]0.5 μM, pH 7.4.

Table 3. Selected Pharmacokinetic Properties of 14[a]

	mouse (10 mg/kg)	rat (5 mg/kg)
	iv[b]	
$T_{1/2}$ (h)	4.6	3.8
V_{ss} (L/kg)	0.3	0.3
Clp (L/h/kg)	0.1	0.05
	po[b]	
$T_{1/2}$ (h)	5.1	5.6
C_{max} (μg/mL)	17.4	9.3
AUC (μg h/mL)	151	130
F (%)	78	91

[a]All values are mean values ± SEMs (n = 3 unless specified otherwise). [b]1% Tween-80 in water.

5 h following the lipid challenge. As demonstrated in Figure 4, oral administration of **14** afforded a sustained reduction in serum triglyceride concentrations throughout the experiment.

The favorable in vitro and pharmacokinetic properties of compound **14** in addition to the potent triglyceride reductions observed in models of postprandial hyperlipidemia prompted further assessment of this compound in acute and chronic secondary pharmacology assays. In a battery of 80 G-protein-coupled receptors, enzymes, and ion channels, **14** showed no inhibition greater than 80% at 10 μM (CEREP). Negligible blockade of the ion channel derived from the human ether-a-go-go-related gene (hERG) gene was observed in a manual patch clamp assay (IC_{50} > 300 μM), and no prolongation of the APD_{90} was observed up to the highest concentration tested in a dog Purkinje fiber repolarization assay. As an assessment of cardiovascular safety, **14** was infused in three ascending doses into comprehensively instrumented anesthetized dogs (n = 6). No physiologically relevant hemodynamic effects were observed through the highest achieved plasma concentration of 20.47 μg/mL. Additionally, no emesis was observed in a ferret model, nor were any changes in GI transit noted in rats through the highest plasma concentrations achieved (30.19 μg/mL). Finally, 2 weeks of oral dosing in rat and dog afforded no significant toxicological findings up to terminal concentrations of 3455 μg h/mL (female) and 789 μg h/mL, respectively.

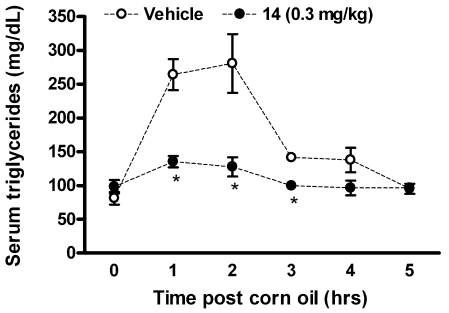

Figure 4. Serum triglyceride concentrations measured in overnight fasted DIO mice pretreated with vehicle or DGAT-1 inhibitor **14** (0.3 mg/kg) prior to and for 5 h after an oral gavage of corn oil (n = 4/group). *p < 0.05 as compared to vehicle.

CONCLUSION

In summary, optimization of the HTS hit **3** lead to the design and preparation of hybrid structure **14**. This compound is a potent and selective inhibitor of DGAT-1 and possesses good oral pharmacokinetics in rodents. Upon oral administration, significant reduction of postprandial triglycerides was observed at doses as low as 0.03 mg/kg in CD-1 mice, and a single dose at 0.3 mg/kg abolished the postprandial triglyceride excursion in DIO mice. Compound **14** shows little cross-reactivity at the hERG channel and other off-targets as assessed by CEREP and no remarkable effects in acute in vivo assays for cardiovascular function, GI transit, and emesis. Similarly, no general toxicology findings were noted up to high plasma levels following prolonged dosing in rat and dog species. As a result of the favorable efficacy and safety profile, compound **14** was advanced to clinical candidacy. A further description of the in vivo profiling in multiple models, cross-species metabolism, and

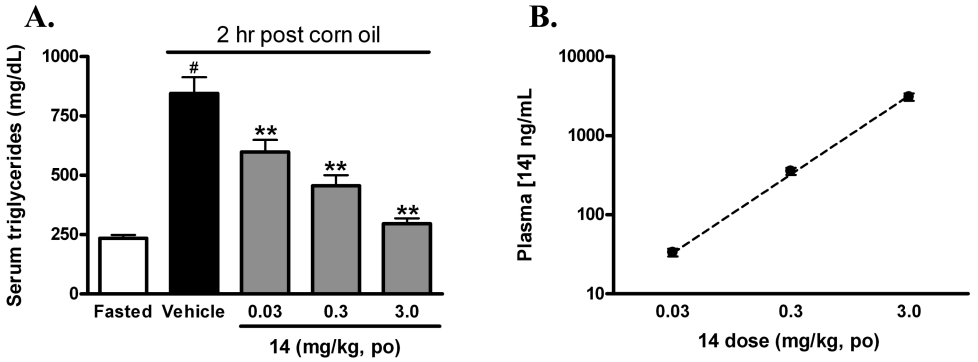

Figure 3. (A) Serum triglyceride concentrations measured in overnight fasted, untreated CD-1 mice and 2 h after an oral gavage of corn oil in mice pretreated with vehicle or DGAT-1 inhibitor **14** at 0.03, 0.3, and 3 mg/kg (n = 10/group). #p < 0.05 as compared to fasted, **p < 0.05 as compared to vehicle. (B) Plasma concentrations of **14** measured 3 h after oral dosing and 2 h after the oral lipid challenge.

dx.doi.org/10.1021/jm201524g | J. Med. Chem. 2012, 55, 1751–1757

projected human pharmacokinetics will be disclosed in due course.

EXPERIMENTAL SECTION

General. Proton NMR spectra were obtained on a Varian Mercury plus 300 or Varian UNITY plus 300 MHz instrument with chemical shifts (δ) reported relative to tetramethylsilane as an internal standard. Target compounds possess a purity of at least 95% based on combustion analysis (<±0.4), performed by QTI (Quantitative Technologies, Inc.). Column chromatography was carried out either with an Analogix IntelliFlash 280 chromatography apparatus using SuperFlash Compound Purification Columns or on silica gel 60 (230−400 mesh). Thin-layer chromatography was performed using 250 mm silica gel 60 glass-backed plates with F254 as indicator.

Ethyl 2-(4-Phenylcyclohexylidene)acetate (15). To a solution of NaO*t*Bu (17.0 g, 176.9 mmol, 1.1 equiv) in THF (100 mL) was added triethyl phosphonoacetate (39.6 g, 176.6 mmol, 1.1 equiv) dropwise over 1 h at 0 °C, and the resulting mixture was stirred at 0 °C for 1 h. A THF (100 mL) solution of 4-phenylcyclohexanone (28.0 g, 160.7 mmol, 1.0 equiv) was then added dropwise over 1 h, and the reaction mixture was warmed to 25 °C and stirred for 90 min. Upon completion of the reaction as indicated by HPLC, heptane (100 mL) and water (100 mL) were added, the contents were mixed for 10 min, and the layers were separated. The organic layer was washed with aqueous $NaHCO_3$ (6.5 wt %, 100 mL) and water (100 mL) and concentrated to a volume of ∼80 mL by rotary evaporation. EtOH (100 mL) was added to the residue, and the resultant solution was reconcentrated to a volume of ∼80 mL by rotary evaporation. This process was repeated to afford an ethanolic solution of ethyl 2-(4-phenylcyclohexylidene)acetate (74.6 g, 52.0 wt %, 38.8 g product, 98% yield against a standard prepared by bulb to bulb distillation (0.2 Torr, 150 °C oven temperature). ^{1}H NMR (400 MHz, $CDCl_3$): δ 7.33−7.10 (m, 5H), 5.67 (s, 1H), 4.15 (q, J = 7.1 Hz, 2H), 4.03−3.92 (m, 1H), 2.77 (tt, J = 12.2, 3.4 Hz, 1H), 2.43−2.27 (m, 2H), 2.10−1.96 (m, 3H), 1.72−1.54 (m, 2H), 1.28 (t, J = 7.1 Hz, 3H). ^{13}C NMR (101 MHz, $CDCl_3$): δ 166.13, 161.22, 145.52, 128.06, 126.41, 125.84, 113.47, 59.60, 44.17, 37.83, 35.72, 34.94, 29.63, 14.61. MS (DCI − NH_3) (M + 18) 262.2 m/e FTIR 2930, 1709, 1647, 1141, 698 cm^{-1}. Anal. calcd for $C_{16}H_{22}O_2$: C, 78.65%; H, 8.25%. Found: C, 78.72%; H, 8.46%.

***trans*-Ethyl 2-4-(4-(Hydroxymethyl)phenyl)cyclohexyl)-acetate (16b).** A solution of ethyl 2-(4-phenylcyclohexylidene)-acetate (38.8 g) in ethanol (200 mL) was hydrogenated over 5% Pd(C) at 50 °C and 40 psi for 2.5 h, filtered, and concentrated by rotary evaporation to a volume of approximately 120 mL to afford a 2.4/1 mixture of *trans* and *cis* isomers. An aqueous solution of LiOH (20.0 g in 100 g water) was added, and the resulting reaction mixture was warmed to 50 ± 5 °C. After 1 h, the *trans* Li-carboxylate crystallized from the reaction mixture as a thick slurry, and additional water (287 g) was added to facilitate mixing, which continued at 50 ± 5 °C for an additional 6 h. Analysis by HPLC revealed that the hydrolysis was complete, and the reaction mixture was cooled to room temperature. The *trans* Li salt was collected by filtration and washed with aqueous 5% LiOH (2 × 50 g). The wet cake was partitioned between EtOAc (250 g) and 6 N HCl (100 g), and the suspension was mixed until all solids were dissolved. After separation of the layers, the EtOAc layer was concentrated by rotary evaporation, and the residue was treated with EtOH (100 g), which was then removed in the same manner. The residue was dissolved in EtOH (300 mL), and H_2SO_4 (0.3 mL) was added. The reaction mixture was heated to reflux and mixed overnight. After this time, HPLC analysis revealed that the re-esterification was complete, and the solution was cooled to room temperature. After it was concentrated to a volume of approximately 60 mL by rotary evaporation, heptane (195 g) was added, the layers were separated, and the organic layer was washed with saturated aqueous $NaHCO_3$ (50 mL) and brine (50 mL). The organic layer was reduced to a volume of approximately 60 mL by rotary evaporation. Heptane (100 g) was added, and the resulting solution was concentrated to ∼60 mL by rotary evaporation affording a heptane solution of **16b** [54.4 g, 46.9 wt %, 25.5 g of product, 94% yield against a standard prepared by bulb to bulb distillation (0.2 Torr, 150 °C oven temperature), ratio 99:1 *trans*- to *cis*-]. ^{1}H NMR (400 MHz, $CDCl_3$): δ 7.31−7.10 (m, 5H), 4.13 (q, J = 7.1 Hz, 2H), 2.46 (tt, J = 12.3, 3.3 Hz, 1H), 2.23 (d, J = 6.7 Hz, 2H), 1.98−1.80 (m, 5H), 1.58−1.42 (m, 2H), 1.26 (t, J = 7.1 Hz, 4H), 1.23−1.07 (m, 2H). ^{13}C NMR (101 MHz, $CDCl_3$): δ 172.43, 146.85, 127.96, 126.45, 125.58, 60.20, 44.22, 42.22, 34.77, 34.09, 33.40, 14.61. MS (DCI − NH_3) (M + 18) 262.2 m/e. FTIR 2923, 1694, 1293, 695 cm^{-1}.

***trans*-Ethyl 2-4-(4-(Hydroxymethyl)phenyl)cyclohexyl)-acetate (17).** To a slurry of $AlCl_3$ (31.2 g, 234 mmol) in dichloromethane (250 mL) was added a solution of ester **16b** in heptanes (54.2 g, 51.1% w/w, 112 mmol) while maintaining the temperature below 5 °C. The flask was again cooled to −5 °C, and oxalyl chloride (17.8 g, 140 mmol) was added while the temperature was maintained below 10 °C. The solution was stirred for 45 min at which time the reaction was complete by HPLC. The reaction mixture was poured slowly into an aqueous solution of $CaCl_2$ (13 g of $CaCl_2$ in 170 mL of water) precooled to −5 °C. The internal temperature of the quench was maintained at or below 10 °C, and the quench solution was stirred at room temperature for 30 min. The organic layer was separated, and the aqueous layer was extracted with DCM (50 mL). The combined organic layers were washed with $CaCl_2$ (13 g $CaCl_2$ in 170 mL of water). The organic layer was then dried over $MgSO_4$ and filtered sequentially through Celite and a carbon-impregnated filter. The solution was concentrated under reduced pressure to 75 g and chased with approximately 250 g of THF to give the product as a 33.7% w/w solution in THF (26.0 g, 79%). ^{1}H NMR (400 MHz, $CDCl_3$): δ 8.05 (d, J = 8.5, 2H), 7.32 (d, J = 8.5, 2H), 4.41 (dd, J = 14.2, 7.11, 2H), 2.61−2.54 (m, 1H), 2.25 (d, J = 6.8, 2H), 1.97−1.85 (m, 4H), 1.57−1.47 (m, 2H), 1.27 (t, J = 7, 3H), 1.24−1.11 (m, 2H). A 250 mL stainless steel pressure canister was charged with THF (19 g, 13 volumes), acid chloride (8.77 g, 16.6% w/w, 4.7 mmol, 1 equiv), triethylamine (2.0 g, 2.75 mL, 19.8 mmol, 2 equiv), and 5% Pd/C (0.62 g) and was agitated for 18 h at room temp under an atmosphere of H_2 (40 psi). The reaction was monitored by HPLC. Upon completion, the catalyst was filtered away using a 0.45 μM filter rinsing with THF (5 g, 3.5 volumes) to give the desired alcohol as a solution in THF (38 g, 3.67% w/w) in 50.1% assay yield. ^{1}H NMR (400 MHz, $CDCl_3$) δ 7.28 (d, J = 8.2, 2H), 7.19 (d, J = 8.2, 2H), 4.65 (s, 1H), 4.13 (dd, J = 7.1, 7.1, 2H), 2.51−2.41 (m, 1H), 2.23 (d, J = 6.7, 2H), 1.93−1.85 (m, 4H), 1.70−1.45 (m, 4H), 1.27 (t, J = 5.0, 3H), 1.22−1.11 (m, 2H).

***trans*-Ethyl 2-4-(4-(Cyanomethyl)phenyl)cyclohexyl)acetate (18).** A solution of alcohol **17** in THF (483 g, 1.79% w/w, 33 mmol) was diluted with MTBE (130 g, 15 volumes) and washed sequentially with 1% Na_2CO_3 aqueous solution (2 × 60 mL), 2 N aqueous solution of HCl (2 × 130 mL), water (2 × 130 mL), and a 5% aqueous NaCl solution (130 mL). The organic layer was dried over $MgSO_4$. The solution was concentrated under reduced pressure to afford an oil that was dissolved in AcOH (26 mL), and a 33% aqueous solution of HBr (13 mL, 3 equiv) was added with stirring. The reaction mixture was stirred for 1.5 h, and the progress was monitored by HPLC. Upon completion of the reaction, water (160 mL) was added slowly to the stirring reaction mixture during which time a brown precipitate formed. The solids were filtered, washed with water (50 mL), 2.5% $NaHCO_3$ (50 mL), and water (50 mL), and dried in an oven overnight at 50 °C to give the desired product as a white solid (8.6 g, 80.9% w/w, 88% yield). ^{1}H NMR (400 MHz, $CDCl_3$): δ 7.3 (d, J = 8.2, 2H), 7.16 (d, J = 8.2, 2H), 4.48 (s, 2H), 4.14 (dd, J = 14.2, 7.1, 2H), 2.52−2.40 (m, 1H), 2.23 (d, J = 6.7, 2H), 1.95−1.83 (m, 5H), 1.57−1.42 (m, 2H), 1.27 (t, J = 7.1, 3H), 1.22−1.09 (m, 2H). A solution of the resultant bromide (10.1 g, 29.9 mmol) in acetonitrile (90 mL) was warmed to 40 °C, and an aqueous solution of NaCN (4.9 g, 100 mmol) in water (10 mL) was added over 15 min while keeping the internal temperature below 50 °C. The reaction mixture was stirred at 40 °C for 6 h. The reaction was monitored by HPLC. Upon completion, the mixture was cooled to room temperature and partitioned between water (225 mL) and MTBE (100 mL). The aqueous layer was separated and extracted with MTBE (60 mL). The

dx.doi.org/10.1021/jm201524g | *J. Med. Chem.* 2012, 55, 1751−1757

combined organic extracts were washed with brine (2 × 100 mL), treated with active charcoal, and filtered through $MgSO_4$ and Celite. The MTBE solution was concentrated to by rotary evaporation, and the residue was crystallized from MTBE/heptane (1/3), filtered, washed with heptane, and dried in a vacuum oven to afford the product as a white crystalline solid (5.7 g, 67%); mp 70−77 °C. ^{1}H NMR (400 MHz, $CDCl_3$): δ 7.25−7.15 (m, 4H), 4.13 (q, J = 7.1 Hz, 2H), 3.69 (s, 2H), 2.47 (tt, J = 12.2, 3.0 Hz, 1H), 2.23 (d, J = 6.8 Hz, 2H), 1.95−1.79 (m, 5H), 1.58−1.42 (m, 2H), 1.26 (t, J = 7.1 Hz, 3H), 1.22−1.09 (m, 2H). ^{13}C NMR (101 MHz, $CDCL_3$): δ 172.24, 146.77, 127.49, 127.13, 126.99, 117.69, 60.12, 43.72, 42.04, 34.58, 33.94, 33.18, 23.35, 14.53. MS (DCI − NH_3) (M + 18) 303.2 *m/e*. FTIR 2918, 2248, 1725, 1160, 826 cm¯1. Anal. calcd for $C_{18}H_{22}NO_2$: C, 75.76%; H, 8.12%. Found: C, 75.78%; H, 8.33%.

***trans*-Ethyl 2-(4-(4-((*Z*)-1-Cyano-2-(dimethylamino)vinyl)-phenyl)cyclohexyl)acetate (19).** To a 250-mL, three-necked, round bottomed flask was charged nitrile **18** (13.4 g, 35.5 mmol), toluene (100 mL), and Bredereck's reagent (20.42 g, 3.3 equiv), and the reaction mixture was heated to 70 °C. The mixture was monitored by HPLC until the starting material was consumed. The reaction mixture was then cooled to 40 °C, and acetic acid (51.04 g, 24 equiv) and 3-aminopyrazole (5.88 g, 2.0 equiv) in 4 mL of CH_3CN were added. The reaction mixture was heated to 75 ± 5 °C for 21 h. The mixture was monitored by HPLC until the starting material was consumed. The acetic acid was then removed by azeotropic distillation with toluene, and the solvent was switched to acetonitrile by concentration and chasing with acetonitrile on the rotary evaporator. The residue was suspended in acetonitrile (200 mL), heated to reflux, and then slowly cooled to 10 °C. The product was collected by filtration and washed with cold acetonitrile (20 mL), cold acetonitrile/water (1/1, 20 mL), and cold water (20 mL). After it was dried in a vacuum oven at 50 °C for 18 h, the product was obtained as a white crystalline solid (10.9 g, 85%); mp 145−147 °C. ^{1}H NMR (400 MHz, DMSO): δ 8.14 − 8.06 (m, 2H), 7.42 (dd, J = 6.3, 1.9 Hz, 4H), 7.33 (d, J = 8.2 Hz, 2H), 6.44 (d, J = 2.3 Hz, 1H), 4.07 (q, J = 7.1 Hz, 2H), 2.58−2.43 (m, 1H), 2.23 (d, J = 6.7 Hz, 2H), 1.91−1.71 (m, 5H), 1.50 (tt, J = 13.5, 6.9 Hz, 2H), 1.27−1.07 (m, 2H), 1.20 (t, J = 7.1 Hz, 3H). ^{13}C NMR (101 MHz, DMSO): δ 171.32, 149.46, 147.55, 145.38, 144.37, 143.29, 131.12, 128.54, 126.86, 101.10, 94.09, 59.49, 43.03, 41.20, 34.04, 33.42, 32.52, 14.30. FTIR 3282, 2920, 1725, 1532, 1091, 772 cm^{-1}. Anal. calcd for $C_{22}H_{26}N_4O_2$: C, 69.82%; H, 6.92%; N, 14.80%. Found: C, 69.88%; H, 7.03%; N, 14.61%.

***trans*-{4-[4-(7-Aminopyrazolo[1,5-*a*]pyrimidin-6-yl)phenyl]-cyclohexyl}acetic Acid (14).** A solution of ester **19** (2.9 g, 7.7 mmol) in THF (35 mL) and MeOH (35 mL) was treated with a solution of NaOH (0.92 g, 23 mmol) at 50 °C for 75 min. After this time, the solution was cooled to room temperature, and the volume was reduced by rotary evaporation to ∼35 mL. The suspension of solids was heated to dissolve the solids and then cooled slowly to 2 °C and held at this temperature for 1.5 h. The solid product was collected by vacuum filtration and washed with water (10 mL). The wet cake was dissolved in water (150 mL) and added slowly to a dilute solution of HCl (0.25 M, 100 mL) at 50 °C. After it was cooled to room temperature, the product was collected, washed with water (10 mL), and dried in a vacuum oven at 50 °C for 18 h. The product (2.1 g, 78%) was obtained as a white crystalline solid; mp 264−266 °C. ^{1}H NMR (400 MHz, DMSO): δ 12.05 (s, 1H), 8.12 (d, J = 2.3 Hz, 1H), 8.10 (s, 1H), 7.44 (s, 2H), 7.38 (dd, J = 36.6, 8.2 Hz, 4H), 6.45 (d, J = 2.3 Hz, 1H), 2.57−2.43 (m, 1H), 2.16 (d, J = 6.9 Hz, 2H), 1.85 (d, J = 11.4 Hz, 4H), 1.76 (ddd, J = 15.6, 11.3, 7.6 Hz, 1H), 1.58−1.41 (m, 2H), 1.21−1.03 (m, 2H). ^{13}C NMR (101 MHz, DMSO): δ 172.99, 149.48, 147.56, 145.47, 144.42, 143.33, 131.11, 128.56, 126.88, 101.15, 94.12, 43.09, 41.47, 33.91, 33.51, 32.65. MS (ESI) (M + 1) 351.3 *m/e* FTIR 3315, 2919, 1702, 1289, 770 cm^{-1}. Anal. calcd for $C_{20}H_{22}N_4O_2$: C, 68.55%; H, 6.33%; N, 15.99%. Found: C, 68.74%; H, 6.59%; N, 15.90%.

DGAT-1 Phospholipid Flasphplate Assay. The inhibition of DGAT-1 was readily determined via a FlashPlate assay. The same procedure was also used to assess activity of compounds against DGAT-2. In this assay, recombinant human DGAT-1 containing an N-terminal His_6-epitope tag was produced in the baculovirus expression system. Insect cells (e.g., *Sf*9 or High Five) were infected for 24−72 h and collected by centrifugation. Cell pellets were resuspended in homogenization buffer [250 mM sucrose, 10 mM Tris-HCl (pH 7.4), and 1 mM EDTA] and lysed using a homogenization apparatus, such as a Microfluidizer (single pass, 4 °C). Cell debris was removed by centrifugation at 10000*g* for 30 min, and microsomal membranes were collected by ultracentrifugation at 100000*g* for 30 min. Mouse DGAT-1 was also produced in insect cells and purified by the same procedures as described above.

The DGAT-1 activity was determined as follows: Assay buffer [20 mM HEPES (pH 7.5), 2 mM $MgCl_2$, and 0.04% BSA] containing 50 μM enzyme substrate (didecanoyl glycerol) and 7.5 μM radiolabeled acyl-CoA substrate.[1-^{14}C]decanoyl-CoA) was added to each well of a phospholipid FlashPlate (PerkinElmer Life Sciences). A small aliquot of membrane (1 μg/well) was added to start the reaction, which was allowed to proceed for 60 min. The reaction was terminated upon the addition of an equal volume (100 μL) of isopropanol. The plates were sealed, incubated overnight, and counted the next morning on a TopCount Scintillation Plate Reader (PerkinElmer Life Science). DGAT-1 catalyzes the transfer of the radiolabeled decanoyl group onto the *sn*-3 position of didecanoyl glycerol. The resultant radiolabeled tridecanoyl glycerol (tricaprin) preferentially binds to the hydrophobic coating on the phospholipid FlashPlate. The proximity of the radiolabeled product to the solid scintillant incorporated into the bottom of the FlashPlate induced fluor release from the scintillant, which was measured in the TopCount Plate Reader. Various concentrations (e.g., 0.0001, 0.001, 0.01, 0.1, 1.0, and 10.0 μM) of the representative compounds were added to individual wells prior to the addition of membranes. The potencies of DGAT-1 inhibition for the compounds were determined by calculating the IC_{50} values defined as the inhibitor concentration from the sigmoidal dose−response curve at which the enzyme activity was inhibited 50%.

In Vivo Characterization. All protocols were approved by the Abbott Laboratories Institutional Animal Care and Use Committee and performed in accordance with the National Institutes of Health Guide for the Care and Use of Laboratory Animals. All animals were housed under standard laboratory conditions with a 12 h light/dark cycle, in a temperature- and humidity-controlled room. Male CD-1 mice were obtained from Charles River Laboratories (Portage, MI). DIO was induced in male C57BL/6J mice (Jackson Laboratories, Bar Harbor, ME) by feeding a high-fat diet [D-12492i (60 kcal% fat) Research Diets] for 18 weeks beginning at 5 weeks of age. After shipment to our facilities, they were acclimated to a pathogen-free barrier facility with a 12 h light/12 h dark cycle, single housed in small mouse shoebox cages with bedding, enrichment, and standard mouse water limits, and were fed the same high-fat diet until reaching greater than 40 g of body weight, usually at the age of 22 weeks. All animals were treated in accordance with IACUC guidelines and the Guide for the Care and Use of Laboratory Animals. Serum triglycerides were measured in the clinical pathology laboratory at Abbott Laboratories on an Aeroset c8000 clinical chemistry analyzer (Abbott Laboratories, Abbott Park, IL) using photometric methods.

Effect of DGAT-1 Inhibition on Postprandial Hyperlipidemia. Either CD-1 or DIO mice were fasted overnight. Animals were randomly assigned to receive either vehicle or DGAT-1 inhibitor 14 at 0.03, 0.3, or 3.0 mg/kg by oral gavage (6 mL/kg). One hour after administration of vehicle or DGAT-1 inhibitor, all animals were given an oral bolus of corn oil (6 mL/kg). Serum triglyceride levels were then measured 2 h later in CD-1 mice and every hour for 5 h in DIO mice.

Statistical Analysis. The effect of DGAT-1 inhibition on postprandial serum triglyceride concentrations was assessed using a one-way ANOVA, with posthoc multiple comparisons made using Dunnett's procedure to compare each dose group (0.03, 0.3, and 3 mg/kg) to the vehicle group.

■ ASSOCIATED CONTENT

Supporting Information

Experimental details for the syntheses of compounds **3**−**11**, in vitro ADME, and pharmacological details/characterization of **14**. This material is available free of charge via the Internet at http://pubs.acs.org.

■ AUTHOR INFORMATION

Corresponding Author

*Tel: 847-937-5312. Fax: 847-935-5165. E-mail: Andrew.souers@abbott.com.

Notes

The authors declare no competing financial interest.

■ ACKNOWLEDGMENTS

We thank Jan Waters for ^{1}H NMR analysis and support and Michael Wendt for valuable discussion.

■ ABBREVIATIONS USED

DGAT, acyl-CoA:diacylglycerol acyltransferase; HTS, high-throughput screen; hDGAT, human DGAT; mDGAT, mouse DGAT-1; BE, binding efficiency; HLM, human liver microsomes; MLM, mouse liver microsomes; hERG, human ether-a-go-go-related gene; DIO, diet-induced obesity

■ REFERENCES

(1) McGarry, J. D. Dysregulation of fatty acid metabolism in the etiology of type 2 diabetes. *Diabetes* **2002**, *51* (1), 7−18.

(2) Yen, C. E.; Stone, S. J.; Koliwad, D.; Harris, C; Farese, R. V. Jr. DGAT enzymes and triacylglycerol biosynthesis. *J. Lipid Res.* **2008**, *49*, 2283−2301.

(3) Cases, S.; Smith, S. J.; Zheng, Y.-W.; Myers, H. M.; Lear, S. R.; Sande, E.; Novak, S.; Collins, C.; Welch, C. B.; Lusis, A. J.; Erickson, S. K.; Farese, R. V. Jr. Identification of a gene encoding an acyl CoA: diacylglycerol acyltransferase, a key enzyme in triacylglycerol synthesis. *Proc. Natl. Acad. Sci.* **1998**, *95* (22), 13018−13023.

(4) Cases, S.; Stone, S. J.; Zhou, P.; Yen, E.; Tow, B.; Lardizabal, K. D.; Voelker, T.; Farese, R. V. Jr. Cloning of DGAT2, a second mammalian diacylglycerol acyltransferase, and related family members. *J. Biol. Chem.* **2001**, *276* (42), 38870−38876.

(5) Smith, S. J.; Cases, S.; Jensen, D. R.; Chen, H. C.; Sande, E.; Tow, B.; Sanan, D. A.; Raber, J.; Eckel, R. H.; Farese, R. V. Jr. Obesity resistance and multiple mechanisms of triglyceride synthesis in mice lacking DGAT. *Nat. Genet.* **2000**, *25*, 87−90.

(6) Chen, H. C.; Smith, S. J.; Ladha, Z.; Jensen, D. R.; Ferreira, L. D.; Pulawa, L. K.; McGuire, J. G.; Pitas, R. E.; Eckel, R. H.; Farese, R. V. Jr. Increased insulin and leptin sensitivity in mice lacking acyl CoA: diacylglycerol acyltransferase 1. *J. Clin. Invest.* **2002**, *109* (8), 1049−1055.

(7) Chen, H. C.; Rao, M.; Sajan, M. P.; Standaerdt, M.; Kanoh, Y.; Miura, A.; Farese, R. V. Jr. Role of adipocyte-derived factors in enhancing insulin signaling in skeletal muscle and white adipose tissue of mice lacking Acyl CoA:diacylglycerol acyltransferase 1. *Diabetes* **2004**, *53* (6), 1445−1451.

(8) Chen, H. C.; Ladha, Z.; Smith, S. J.; Farese, R. V. Jr. Analysis of energy expenditure at different ambient temperatures in mice lacking DGAT-1. *Am. J. Physiol. Endocrinol. Metab.* **2003**, *284* (1), E213−218.

(9) Buhman, K. K.; Smith, S. J.; Stone, S. J.; Repa, J. J.; Wang, J. S.; Knapp, F. F. Jr.; Burri, B. J.; Hamilton, R. L.; Abumrad, N. A.; Farese, R. V. Jr. DGAT-1 is not essential for intestinal triacylglycerol absorption or chylomicron synthesis. *J. Biol. Chem.* **2002**, *277* (28), 25474−25479.

(10) Smith, R.; Campbell, A.; Coish, P.; Dai, M.; Jenkins, S.; Lowe, D.; O'Connor, S.; Su, N.; Wang, G.; Zhang, M.; Zhu, L. Preparation and use of aryl alkyl acid derivatives for the treatment of obesity. US2005/07091228.

(11) Fox, B. M.; Furukawa, N. H.; Hao, X.; Lio, K.; Inaba, T.; Jackson, S. M.; Kayser, F.; Labelle, M.; Kexue, M.; Matsui, T.; McMinn, D. L.; Ogawa, N.; Rubenstein, S. M.; Sagawa, S.; Sugimoto, K.; Suzuki, M.; Tanaka, M.; Ye, G. Yoshida, A.; Zhang, J. A. Preparation of fused bicyclic nitrogen containing heterocycles, useful in the treatment or prevention of metabolic and cell proliferative diseases. WO 2004/047755A2, CAN 141:38623.

(12) Birch, A. M.; Buckett, L. K.; Turnbull, A. V. DGAT1 inhibitors as anti-obesity and anti-diabetic agents. *Curr. Opin. Drug Discovery Dev.* **2010**, *13* (4), 489−496.

(13) Dow, R. L.; Li, J.-C.; Pence, M. P.; Gibbs, E. M.; LaPerle, J. L.; Litchfield, J.; Piotrowski, D. W.; Munchhof, M. J.; Manion, T. B.; Zavadoski, W. J.; Walker, G. S.; McPherson, R. K.; Tapley, S.; Sugarman, E.; Guzman-Perez, A.; Dasilva-Jardine, P. Discovery of PF-04620110, a Potent, Selective, and Orally Bioavailable Inhibitor of DGAT-1. *ACS Med. Chem. Lett.* **2011**, *2*, 407−412.

(14) http://clinicaltrials.gov/ct2/show/NCT01146522?term=LCQ-908&rank=1.

(15) Zhao, G.; Souers, A. J.; Voorbach, M.; Falls, H. D.; Droz, B.; Brodjian, S.; Lau, Y. Y.; Iyengar, R. R.; Gao, J.; Judd, A. S.; Wagaw, S. H.; Raven, M. M.; Engstrom, K. M.; Lynch, J. K.; Mulhern, M. M.; Freeman, J.; Dayton, B. D.; Wang, X.; Grihalde, N.; Fry, D.; Beno, D. W. A.; Marsh, K. C.; Su, Z.; Diaz, G. J.; Collins, C. A.; Sham, H.; Reilly, R. M.; Brune, M. E.; Kym, P. R. Validation of diacyl glycerolacyl-transferase 1 as a novel target for the treatment of obesity and dyslipidemia using a potent and selective small molecule inhibitor. *J. Med. Chem.* **2008**, *51*, 380−383.

(16) King, A. J.; Segreti, J. A.; Larson, K. J.; Souers, A. J.; Kym, P. R.; Reilly, R. M.; Zhao, G.; Mittelstadt, S. W.; Cox, B. F. Diacylglycerol acyltransferase 1 (DGAT-1) inhibition lowers serum triglycerides in the Zucker fatty rat and the hyperlipidemic hamster. *J. Pharmacol. Exp. Ther.* **2009**, *330* (2), 526−531.

(17) King, A. J.; Segreti, J. A.; Larson, K. J.; Souers, A. J.; Kym, P. R.; Reilly, R. M.; Collins, C. A.; Voorbach, M. J.; Zhao, G.; Mittelstadt, S. W.; Cox, B. F. In vivo efficacy of acyl CoA:diacylglycerol acyltransferase (DGAT) 1 inhibition in rodent models of postprandial hyperlipidemia. *Eur. J. Pharmacol.* **2010**, *637* (1−3), 155−161.

(18) Abad-Zapatero, C.; Metz, J. M. Ligand efficiency indices as guideposts for drug discovery. *Drug Discovery Today* **2005**, *10*, 464−469.

(19) Nassar, A-E. F.; Kamel, A. M.; Clarimont, C. Improving the decision-making process in the structural modification of drug candidates: enhancing metabolic stability. *Drug Discovery Today* **2004**, *9*, 1020−1028.

(20) An additional example of improving pharmacokinetic properties via the incorporation of carboxylic acid groups into a DGAT-1 inhibitor can be found in the following reference: Qian, Y.; Wertheimer, S. J.; Ahmad, M.; Cheung, A. W.; Firooznia, F.; Hamilton, M. M.; Hayden, S.; Li, S.; Marcopulos, N.; McDermott, L.; Tan, J.; Yun, W.; Guo, L.; Pamidimukkala, A.; Chen, Y.; Huan, K.; Ramsey, G. B.; Whittard, T.; Conde-Knape, K.; Taub, R.; Rondinone, C. M.; Tilley, J.; Bolin, D. Discovery of orally active carboxylic acid derivatives of 2-phenyl-5-trifluoromethyloxazole-4-carboxamide as potent diacylglycerol acyltransferase-1 inhibitors for the potential treatment of obesity and diabetes. *J. Med. Chem.* **2011**, *54*, 2433−2446.

(21) Birch, A. M.; Birties, S.; Buckett, L. K.; Kemmitt, P. D.; Smith, G. J.; Smith, T. J.; Turnbull, A. V.; Wang, S. J. Discovery of a potent, selective, and orally efficacious pyrimidinooxazinyl bicyclooctaneacetic acid diacylglycerol acyltransferase-1 inhibitor. *J. Med. Chem.* **2009**, *52* (6), 1558−1568.